We are IntechOpen, the world's leading publisher of Open Access books
Built by scientists, for scientists

6,900
Open access books available

186,000
International authors and editors

200M
Downloads

Our authors are among the

154
Countries delivered to

TOP 1%
most cited scientists

12.2%
Contributors from top 500 universities

CLARIVATE ANALYTICS
BOOK CITATION INDEX
INDEXED

WEB OF SCIENCE™

Selection of our books indexed in the Book Citation Index
in Web of Science™ Core Collection (BKCI)

Interested in publishing with us?
Contact book.department@intechopen.com

Numbers displayed above are based on latest data collected.
For more information visit www.intechopen.com

Simulation of Tunnel Surrounding Rock Mass in Porous Medium with Hydraulic Conductivity Tensor

Lin-Chong Huang and Cui-Ying Zhou
Sun Yat-sen University
China

1. Introduction

The deformation of surrounding rock in tunnel is a comparatively complex process, because of the heterogeneous and discontinuous characters in deformation, which belongs to a highly nonlinear problem.

In recent years, many researchers have paid a lot of attention to the study of deformation in the soft surrounding rock. Sulem(1987) and Stille(1989) got the analytic solution of displacement under the hydrostatic pressure state. In fact, this result is based the linear yield criterion in the condition of small deformation. According the experiments, Lade(1977), Agar(1985), and Santarelli(1987) pointed out that, in soft surrounding rock, especially in the soft soil, the relationship between the maximum principle and the minimum stresses is nonlinear, and the linear relationship is only just the special case. In 1966, Hobbs proposed the Power law nonlinear criterion for the fist time, and then Ladanyi suggested a new nonlinear criterion from the crack theory of Griffith in 1974. Kennedy and Linderg studied it using the segment linear theory in 1978, and Brown got the Hoek-Brown nonlinear failure criterion based on predecessors.

With the rapid development of computing power, extensive research has been done on the 3D modeling of tunnel construction. In addition to the special issue on tunneling mentioned earlier, Shahrour and Mroueh(1997) performed a full 3D FEM simulation to study the interaction between tunneling in soft soils and adjacent surface buildings. Their analysis indicated that the tunneling-induced forces largely depended on the presence of the adjacent building and neglecting of the building stiffness in the tunneling-structure analysis yielded significant over-estimation of internal forces in the building members. Tsuchiyama et al. (1988) analysed the deformation behaviour of the rock mass around an unsupported tunnel intersection in the construction of a new access tunnel to the existing main tunnel using 3D linear elastic FEM and found that the influence area along the main tunnel was on the order of one tunnel diameter on the obtuse angle side and about three times the tunnel diameter on the acute angle side from the point of intersection. Rowe and Kack(1983) carried out a numerical analysis based on the finite element method and compared the results with case histories for predicting and designing the settlement above tunnels constructed in a soft ground. Kasper and Meschke(2004) developed a 3D finite element model for a shield-driven tunnel excavation in a soft ground and reproduced settlement, pore pressure distribution, stress levels, and deformations in the lining and in the soil.

Constitutive modeling is an important aspect for the analysis of the displacement and stress fields. A review of existing literature suggests that elastoplastic theory seems to be the most popular framework for constitutive modeling. Borja et al. (1997) formulated the problem of elastoplastic consolidation at finite strain. They showed that for saturated soil media with incompressible solid grains and fluids, balance of energy suggests that Terzaghi's effective stress was the appropriate measure of stress for describing the constitutive response of the soil skeleton. Consequently, the formulation had the advantage of being able to accommodate a majority of the effective stress-based models developed in geotechnical engineering for describing the deformation behaviour of compressible clays. Elastoplastic analyses of circular tunnels excavated in Mohr-Coulomb media have been performed by numerous investigators. For elastic brittle plastic case, Brown et al. (1983) presented the closed-form solution for stress and radial displacement in the plastic zone. However, they did not consider the variation of elastic strain, resulting in the neglect of the influence of the unloading in the plastic zone. Recently, several improved solutions were provided. An analytical solution for Hoek–Brown rock mass given by Sharan(2005) was not exact in calculating displacements in plastic zone, as it was assumed that the elastic strain field in the plastic zone was the same as that of thickwall cylinder problem. Solutions by Park and Kim (2006) offered an exact expression for displacement in the plastic zone.

To sum up, most of the research efforts on tunneling to date have focused on the assessment of the ground surface settlement although some have begun to pay attention to the interaction between tunneling and existing surface structures such as adjacent buildings. Relatively, little research work can be found in the literature on the particular constitutive model for soft soil, especially for the tunnel in porous medium. Also, in the numerical modeling, the Finite Difference Method (FDM) is seldom used in the simulation. The purpose of this paper is to present an elastoplastic model with hydraulic conductivity tensor perform utilizing FLAC3D, and monitor the mechanical behaviour of the tunnel deformation response in the porous medium tunnel during construction.

2. Constitutive model framework

There is the need to establish a link between the state of stresses and the deformations, also a link between the flow vector and the fluid pressure in soft argillaceous shale tunnel. In these links, the stresses are assumed to be a nonlinear function of the deformation via an elastoplastic constitutive response.

The deformation of the surrounding rock includes elastic and plastic deformation in elastoplastic model theory, thus we should set up the constitutive model by combining elastic and plastic theory. In the constitutive relation, there are Mohr-Coulomb and Drucker-Prager yield criterions for the surrounding rock material.

As showed in Fig. 1, when friction angle φ >0, the yield surface of the Drucker-Prager criterion is a conical surface in the principal stress space, which is inscribed at the Mohr-Coulomb yield surface; while if φ =0, the Drucker-Prager criterion is exactly the Mises criterion.

3. Deformation numerical simulation in soft argillaceous shale tunnel

The Guan Kouya tunnel is taken as the research objection here, which is a typical soft argillaceous tunnel located at Hunan province in China. It is a four-lane bidirectional

separated tunnel with 880m in length. The geologic investigation data show that the rock is mainly soft argillaceous shale with distinct stratification structure, and the surrounding rock is classified as IV and V. The structure is supervised by NATM, and the support obtains the composite lining, with anchor and sprayed concrete to be the primary support together with the reinforced concrete as the secondary lining.
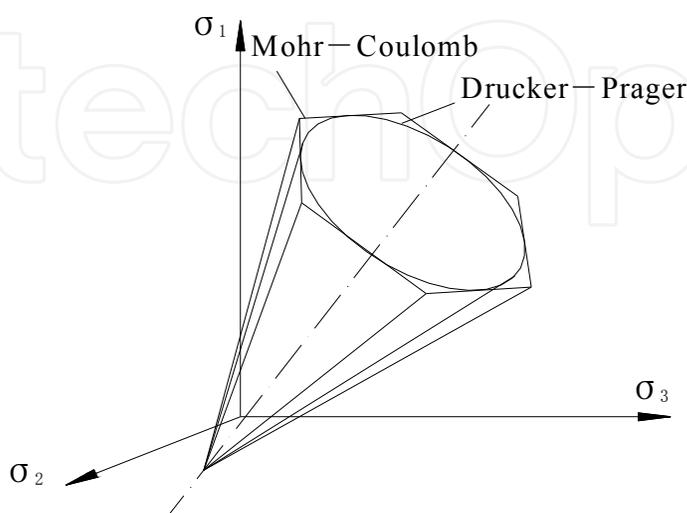

Fig. 1. Mohr－Coulomb & Drucker－Prager yield surface

3.1 Computational model

In order to obtain the deformation characters and compare them with the measurement results in site, using the software FLAC3D, the typical cross section (YK73+839.5, classified as V) is simulated and computated, which is exactly the section measured in site.

3.1.1 Computational bound

The boundary of the computational model is more than three times of the cavity width in each direction, so that the adverse influnce caused by the boundary constraint condition can be reduced sharply in the process of computation. To be specific, the computational zone includes $100\,m$ in the horizontal direction, $30\,m$ from the arch head to the ground in the vertical direction, and $30\,m$ along with the route direction, which can be clearly observed in Fig. 2. The water height is 5.6m over the arch crown.
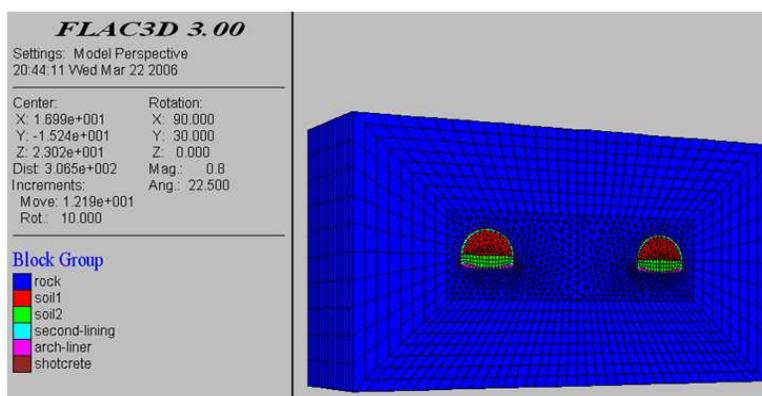

Fig. 2. Numerical computation model

3.1.2 Anchor simulation

It is unrealistic to simulate each anchor in computation, because there are so many anchors in the three-dimensional model. There is an effective method to solve this problem shown in [Huang, 2009] by enhancing the cohesive force instead of the effection of anchoring. The equation of the cohesive force in the anchoring rock is shown as:

$$C = C_0 \left[1 + \frac{\eta}{9.8} \cdot \frac{\tau S_m}{ab} \times 10^4 \right] \tag{1}$$

Where C_0 and C are the cohesive forces before and after adding the anchor(MPa), respectively; τ is the maximum shear stress of the anchor(MPa); S_m is the acreage of the anchor (m^2); a and s are the distances between each other in the longitudinal and lateral directions, respectively (m); η is a empirical coefficient, and it equals 4.0 in this project.
The material parameters utilized in the simulation is summarized in Table 1.

Items	R (kN/m^3)	E (GPa)	μ	C (kPa)	ϕ ($^\circ$)
soft argillaceous shale	2.0	1	0.45	10	31
C25 concrete	23	29.5	0.2	—	—
C30 concrete	23	31	0.2	—	—

Table 1. Summary of simulation papameters

3.1.3 Construction procedure

This structure is simulated as two separate sigle cavities. We obtain the "bench method" in computational simulation, just as the method used in the pratical construction phases, and the procedures are followed as:
step 1→excavating $5\,m$ in the upper bench and setting primary support; Step 2→excavating $5\,m$ in the upper bench additionally and setting primary support, at the same time, excavating $5\,m$ in the lower bench and setting primary support; Step 3→setting the secondary support; Step 4→excavating $5\,m$ in the upper bench and setting primary support, at the same time, excavating $5\,m$ in the lower bench and setting primary support. The construction simulation is done according to this flow operation.
In order to compare the computational results with the measurement data in site conveniently, some typical locations are chosen to be computated and analyzed, and these locations are the same as those measured in site. The construction procedure and these typical locations are shown in Fig. 3.

3.2 Deformation analysis

The maximum computational displacement results of the typical locations around the cavity are summarized in Table 2, and the displacement convergence of the arch crown at cross section YK73+839.5 is shown in Fig. 4.
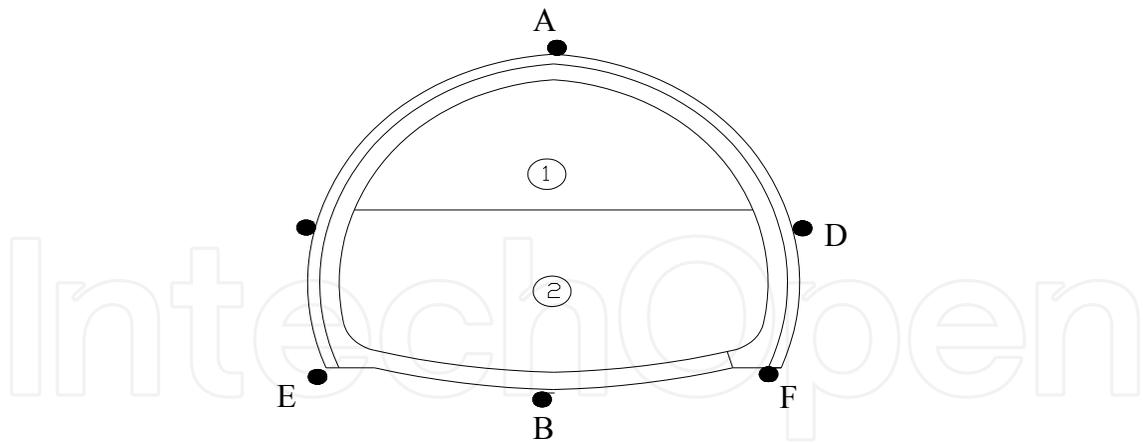
Fig. 3. Typical location & construction procedure

Construction phase	Vertical displacement of the typical locations（mm）					
	A	C	E	B	F	D
Step 1	-37.853	-22.046	-13.091	11.276	-13.581	-24.482
Step 2	-38.518	-12.091	-13.528	11.143	-13.170	-27.905
Step 3	-39.175	-22.975	-14.039	10.791	-14.786	-31.044
Note: minus means the displacement direction downwards.						

Table 2. Displacement computation results of the typical locations around the cavity
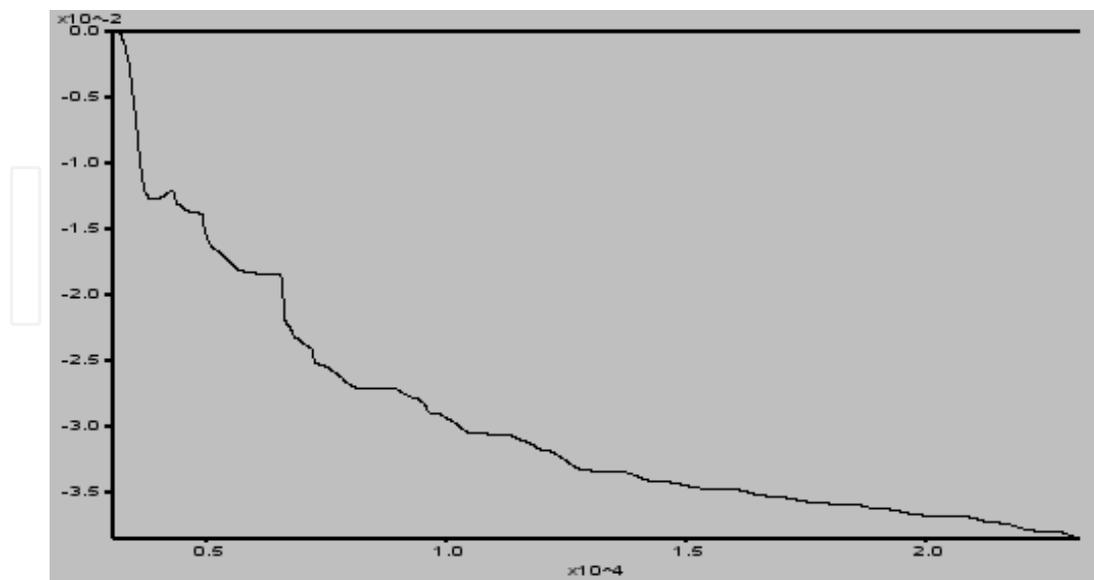
Fig. 4. Displacement convergence of arch crown (Unit:m)

The relative displacements at the arch crown (point A) in section YK73+839.5 are plotted in Figure 5.
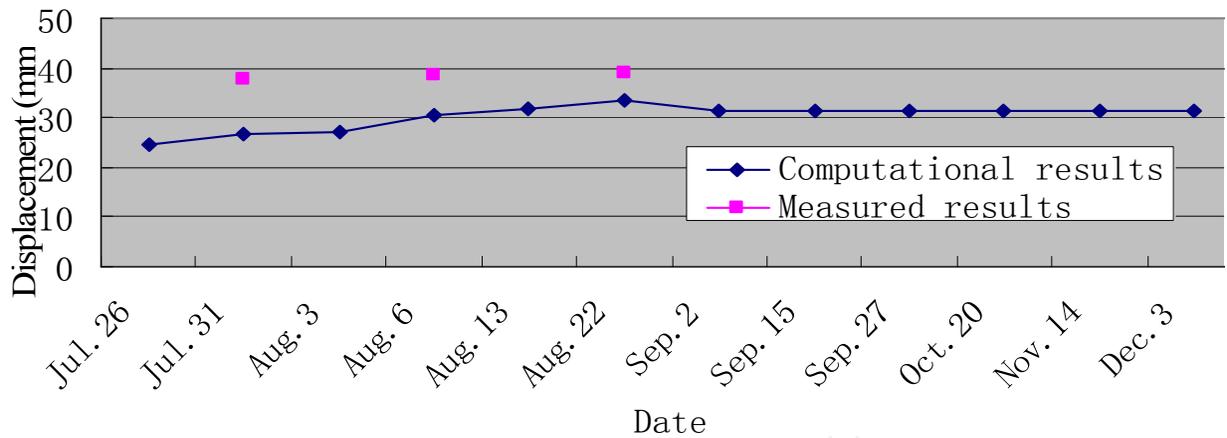
Fig. 5. Graph of the relative displacement change at the arch crown (point A)

While the relative displacements at the right of arch springing (point F) in section YK73+839.5 are plotted in Figure 6.
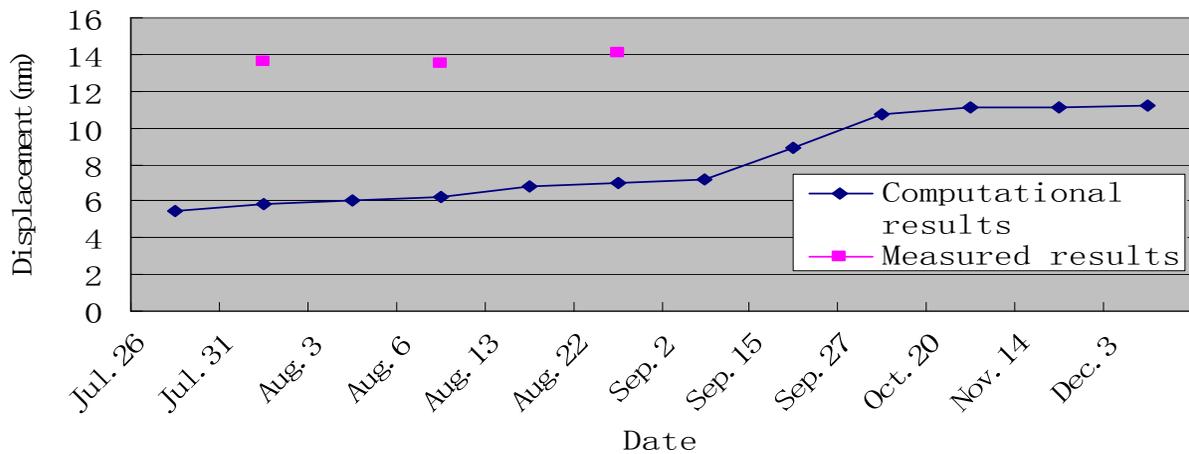
Fig. 6. Graph of the relative displacement change at the arch spinging (point F)

The computational results and the measured results of some typical points are comparatively summarized in Table 3.(Noting that the Graph of the relative displacements at the left arch springing (point E) is elided)

Result	Left arch springing（E）	Arch crown (A)	Right arch springing (F)
Computational value	14.039	39.175	14.786
Measured value	10.02	31.16	11.19

Table 3. Internal displacement value of the section YK73+839.5 (Unit：mm)

The comparative analysis about the computational and the measured results are followed below.

Computational results analysis:

1. The deformaion velocity is much high in the beginning, compared with the late phase, while the time that the deformation get steady is much long. These laws are coincident with the data measured in site.

2. The displacement convergence at the arch crown is 0.51576% after the construction of the secondary lining, while it is 0.6504% at the arch. Spingring. Both of the convergence values are much large, but are not beyond the allowable values, which are less than 0.4%~1.2%. At this point, evaluating with the displacement convergence, this tunnel is steady under constructrue howbeit the convergence values are large. These laws are also coincident with the data measured in site.

Measured results analysis:

1. The deformation velocity rises rapidly in the first 6 days, and goes to steady state after 40 days.
2. The displacement at the arch crown get steady after 30 days, which shows that the deformaion velocity is much high, and the time that the deformation get steady is also much long
3. The displacement at the arch spinging goes to steady state after 40 days, at which point the time is longer than the arch crown.
4. The vertical displacement of the arch spinging increases at all time, and the displacement at the arch crown are always larger than the arch spinging. This rule is also coincident with the computational results.

3.3 Plastic zone analysis

Figure 7 and 8 show the plastic zone of the computational section after excavating the upper bench and the lower bench, respectively, where "shear-n" means failure, while "shear-p" means yielding but no failure.

The plastic zone is small after step 2, in which tension and shearing yield appears in few zone. The whole initial support is almost in a state of "yield" before the construction of the secondary lining, which takes the form of the so-called "pulling yield" from the middle to the bottom of the arch, whereas it appears as the so-called "shear yield" in the 3~4 m near the excavating surface and the arch spinging. These suggest that the secondary lining and the Invert should be set in time during the construction of soft surrounding rock tunnel, so that the closed support can be formed in time, which is especially important to insure the tunnel safety, which are shown in Figure 7 and 8.
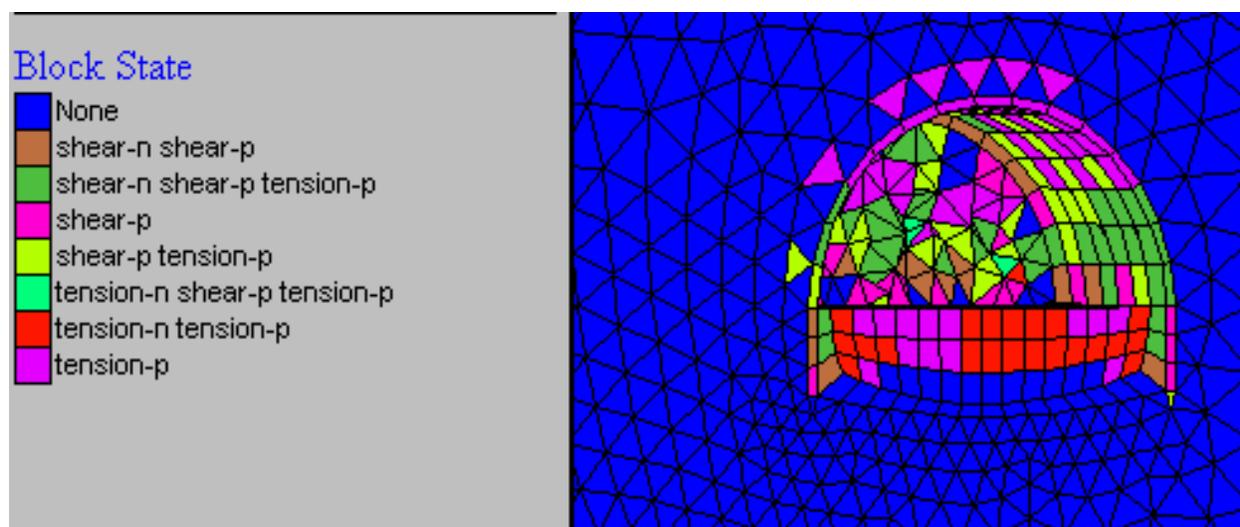

Fig. 7. Distributing of the plastic region
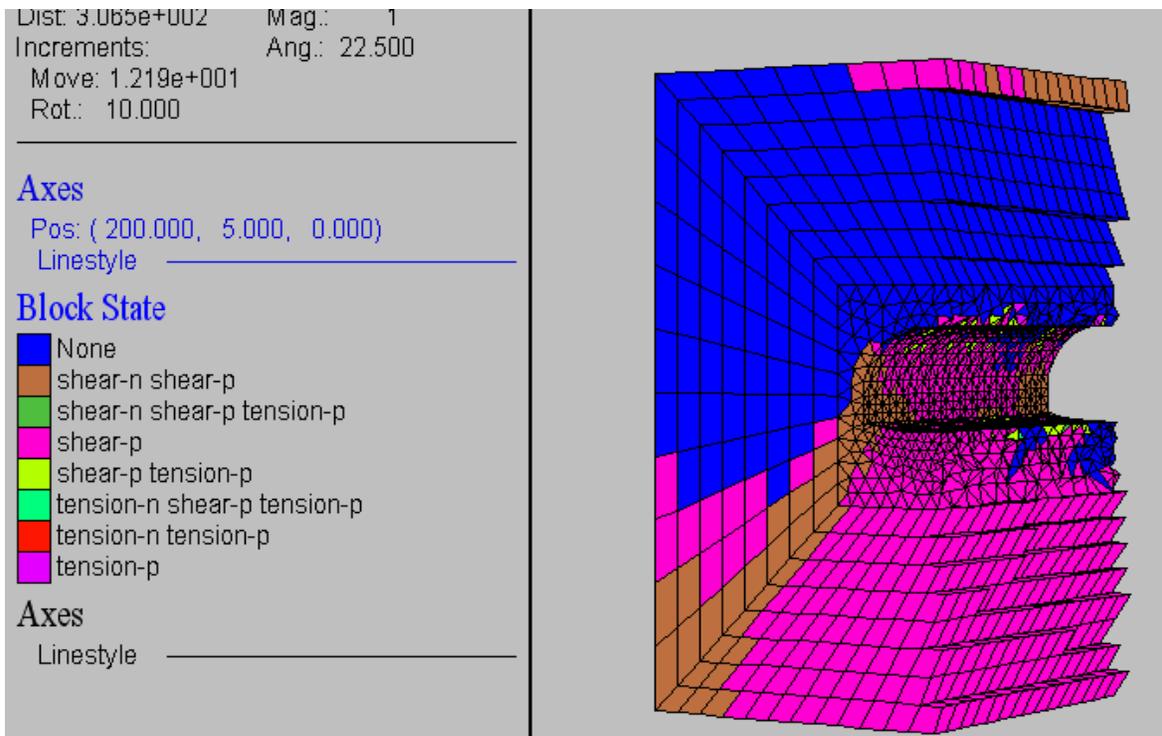
Fig. 8. Portrait distributing of the plastic region

3.4 Secondary lining stress analysis

Figure 9 and 10 show the maximum and minimum principle stresses of the computational values, respectively, while the the maximum and minimum principle stresses of the typical points can be clearly observed in Table 4.
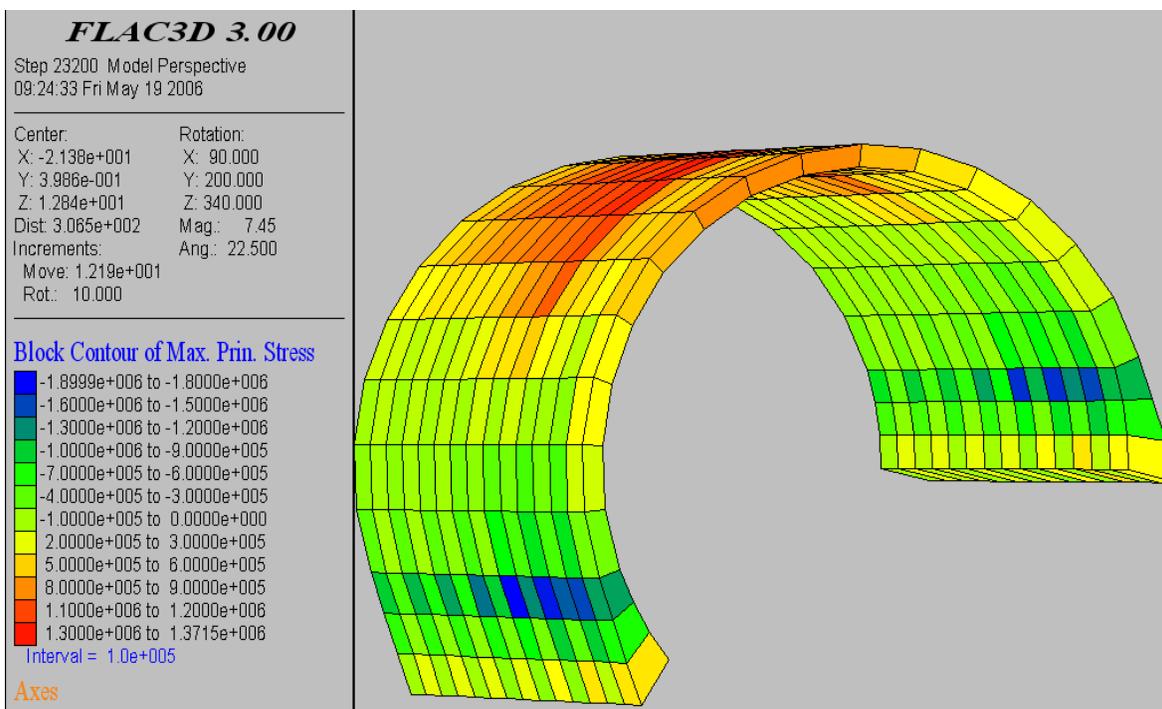

Fig. 9. Maximum main stress of the 2ed lining (Unit:Pa)
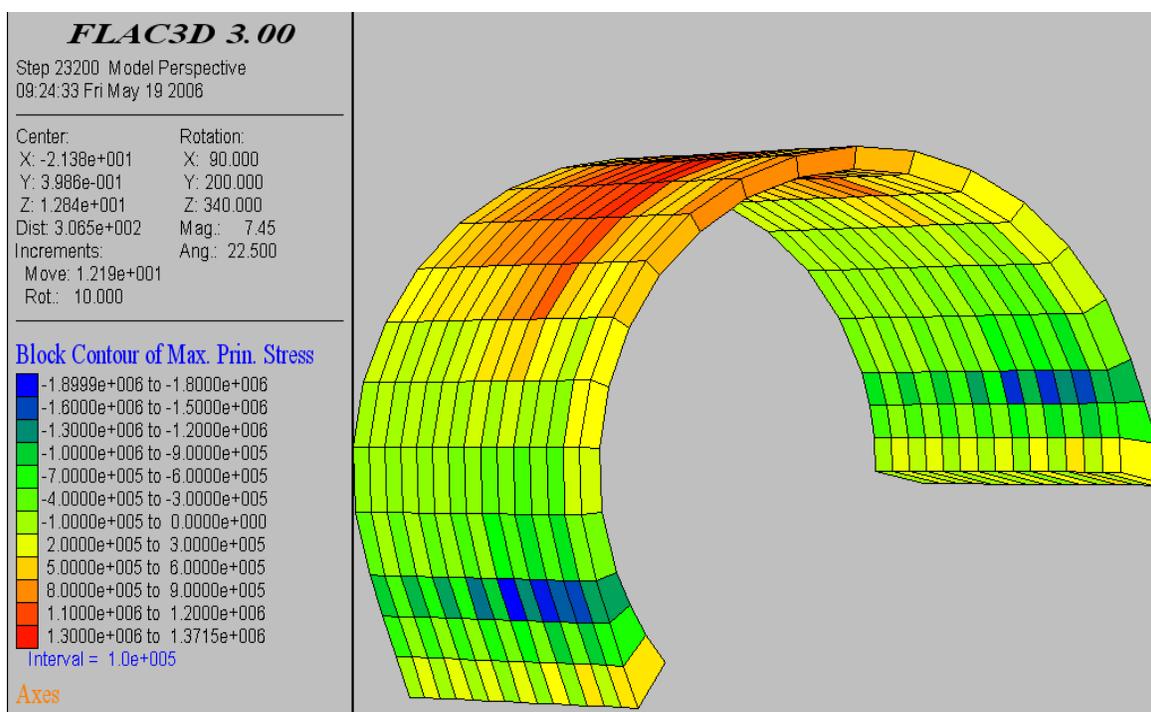
Fig. 10. Maximum main stress of the 2ed lining (Unit:Pa)

Item	A	C	E	B	F	D
Maximum principle stress（MPa）	6.50	4.16	9.91	None	10.76	10.06
Minimum principle stress (MPa)	-0.11	-0.19	-0.39	None	-1.34	-1.76
Note: The minus means tension stress.						

Table 4. The max. & min. principle stress of the typical locations at the secondary lining

Some results can be obtained from the computation such that: There are mainly pression stress in secondary lining, and the maximum pression stress is 10.76 $_{MPa}$, which is located at the middle of the arch, at the same time, which is 44.46% of the designed concrete compressive strength. At this point, the secondary lining is steady. However, there are few tension stresses near the arch spinging, and the maximum is 1.76 $_{MPa}$, 88% of the designed concrete tensile strength, which suggests some reinforcing steel bars should be configured.

Table 5 shows the internal force values of the locations at secondary lining according to the measrued data, from which, we get the shematic diagram of the axial force and moment, shown as Figure 11 and 12, respectively.

Some results can also be suggested from the measured data, i.e.:

1. In the secondary lining, the initial stresses are mostly the tension, because of the contractive stress of the concrete in the prophase. However, they will trun to be the compressive stresses about one month later, in particular, these compressive stresses increace slowly with the time, which will be steady about two months later.

2. The secondary lining moment is much high at the arch crown and the arch spinging, which is basiclly coincident with the mechanical characteristic of the mold casting lining.

location	axial force (KN)	moment (KN·m.)
A	542	11
C	262	4.6
E	678	-9.5
D	433	1.3
F	981	-5.3

Table 5. Internal force results of the measure locations at the secondary lining
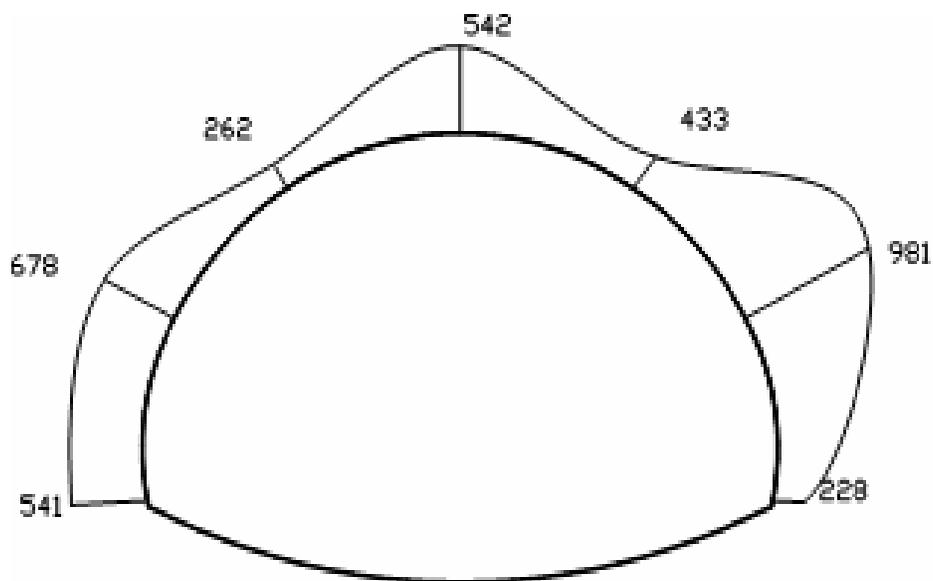
Fig. 11. Sketch map of axial force in 2ed lining (unit: KN)
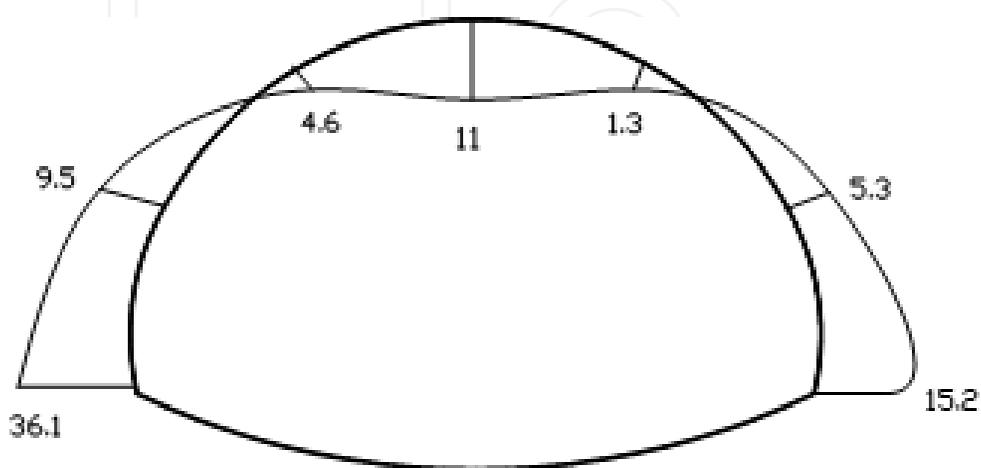
Fig. 12. Sketch map of moment in 2ed lining (unit: KN· m)

4. Conclusion

We have presented a nonlinear finite element model for the simulation of the tunnel in porous medium with hydraulic conductivity tensor. Using the FLAC3D code, the numerical simulation analysis is done to the Guan Kouya soft argillaceous shale tunnel .Some results are obtained, compared with the measurement data in site, such that:

1. The deformation velocity is fast during the prophase of the tunnel excavating, compared with the later phase, but the steady time remains long;
2. Regarding the vertical displacement, the displacement of the arch crown appears bigger than that of the middle, while the displacement of the arch springing is the least obvious, and the horizontal displacement always remains small;
3. The whole initial support is almost in a state of "yield" before the construction of the secondary lining, which takes the form of the so-called "pulling yield" from the middle to the bottom of the arch, whereas it appears as the so-called "shear yield" in the 3~4m near the excavating surface and the arch. These suggest that the secondary lining and the Invert should be set in time during the construction of soft surrounding rock tunnel, so that the closed support can be formed in time, which is especially important to insure the tunnel safety;
4. The surrounding rock stress releases rapidly after the excavating of the cavity, at this point, some assistant methods, especially the lock-foot anchor should be applied to enhance the steady stability due to the big compressive stress located at the arch of the two sides in the tunnel.

5. Acknowledgment

6. References

Sulem, J. ; Panet, M. & Guenot, A (1987). An analytical solution for time-dependent displacement in a circular tunnel. *Int J. Rock Mech Mi Sci & Geomech Abstr*, Vol.24, No.3,pp. 155-164.

Stille, H. ; Holmoery, M. & Mord, G(1989). Support of week rock with grouted bolts and shoterete. *Int J Rock Mech Mi Sci & Geomech Abstr*, Vol.26, No.1,pp. 99-103.

Lade, P. V. (1977). Elasto plastic stress strain theory for cohesionless soil with curved yield surface. *Int J Skilds Struct*, Vol.13, pp. 1019-1035.

Agar, J. G. ; Morgensteren, N. R. & Scott, J. Shear strength and stress strain behaviour of Athabasca oil sand at elevated temperatures and pressure (1985). *Can. Geotech. J.*, Vol.24, No.1, pp. 1-10.

Santarelli, F. Theoretical and experimental investigation of the stability of the axisy metric borehole(1987). University of London.

Shahrour, I. & Mroueh, H.(1997). Three-dimensional non linear analysis of a closely twin tunnels. *Sixth International Symposium on Numerical Models in Geomechanics*, Montreal, pp. 481-487.

Tsuchiyama, S. ; Hayakawa, M. ; Shinokawa, T. & Konno, H.(1988). Deformation behaviour of the tunnel under the excavation of crossing tunnel. *Proceedings of the 6th International Conference on Numerical Methods in Geomechanics*, Innsbruck, pp. 1591-1596.

Rowe, R.K. & Kack, G.J(1983). A theoretical examination of the settlements induced by tunneling four case histories. *Can. Geotech. J.*, Vol.20, pp, 299-314.

Kasper, T. & Meschke, G.(2004). A 3D finite element simulation model for TBM tunneling in soft ground. *Int. J. Numer. Anal. Meth. Geomech.*, Vol.28, pp, 1441-1460.

Borja, R.I. & Andrade, J.E.(2006). Critical state plasticity, Part VI: Meso-scale finite element simulation of strain localization in discrete granular materials. *Computer Methods in Applied Mechanics and Engineering*, Vol.195, pp, 5115-5140.

Borja, R.I.; Tamagnini, C. & Amorosi, A.(1997). Coupling plasticity and energy conserving elasticity models for clays, *J. Geotech. Geoenviron. Engrg.*, Vol.123, pp, 948-957.

Brown, E.T. ; Bray, J.W ; Ladanyi, B. & Hoek, E.(1983). Ground response curves for rock tunnels. *J. Geotech. Eng., ASCE,* Vol.109, pp, 15 – 39.

Huang, L.C, Xu, Z.S, Wang, L.C. Constitutive equations and finite element implementation of strain localization in sand deformation(2009). Journal of Central South University of Technology. Vol.16,No.3, pp, 482-487

Sharan, S.K.(2005). Exact and approximate solutions for displacements around circular openings in elastic – brittle – plastic Hoek – Brown rock. *Int. J. Rock Mech. Min. Sci.* Vol.42, pp, 542-549.

Park, K.H. & Kim, Y.J.(2006). Analytical solution for a circular opening in an elasto-brittle-plastic rock. *Int. J. Rock Mech. Min. Sci.* Vol.43, pp, 616-622.

Kumar, P. (2000). Infinite Elements for Numerical Analysis of Underground Excavations[J]. Tunneling and Underground Space Technology, Vol.15, No.1, pp, 117-124.

Earth and Environmental Sciences

Edited by Dr. Imran Ahmad Dar

We are increasingly faced with environmental problems and required to make important decisions. In many cases an understanding of one or more geologic processes is essential to finding the appropriate solution. Earth and Environmental Sciences are by their very nature a dynamic field in which new issues continue to arise and old ones often evolve. The principal aim of this book is to present the reader with a broad overview of Earth and Environmental Sciences. Hopefully, this recent research will provide the reader with a useful foundation for discussing and evaluating specific environmental issues, as well as for developing ideas for problem solving. The book has been divided into nine sections; Geology, Geochemistry, Seismology, Hydrology, Hydrogeology, Mineralogy, Soil, Remote Sensing and Environmental Sciences.

INTECH
open science | open minds